iScience

Article

Bacterially Derived Tryptamine Increases Mucus Release by Activating a Host Receptor in a Mouse Model of Inflammatory Bowel Disease

Yogesh Bhattarai,
Si Jie, David R.
Linden, ...,
Gianrico Farrugia,
Lei Sha, Purna C.
Kashyap

lei.sha@foxmail.com (L.S.)
kashyap.purna@mayo.edu
(P.C.K.)

HIGHLIGHTS

Tryptamine increases serotonin-receptor4-dependent colonic mucus release

Bacterially derived tryptamine attenuates weight loss in DSS colitis mouse model

Protective effect of tryptamine in DSS colitis is more pronounced in female mice

Tryptamine reduces colitis severity and barrier disruption specifically in female mice

iScience

Article

Bacterially Derived Tryptamine Increases Mucus Release by Activating a Host Receptor in a Mouse Model of Inflammatory Bowel Disease

Yogesh Bhattarai,[1,6] Si Jie,[1,6] David R. Linden,[2] Sayak Ghatak,[1] Ruben A.T. Mars,[1] Brianna B. Williams,[3] Meng Pu,[1] Justin L. Sonnenburg,[4] Michael A. Fischbach,[3] Gianrico Farrugia,[1,2] Lei Sha,[5,*] and Purna C. Kashyap[1,2,7,*]

SUMMARY

Recent studies emphasize the role of microbial metabolites in regulating gastrointestinal (GI) physiology through activation of host receptors, highlighting the potential for inter-kingdom signaling in treating GI disorders. In this study, we show that tryptamine, a tryptophan-derived bacterial metabolite, stimulates mucus release from goblet cells via activation of G-protein-coupled receptor (GPCR) 5-HT4R. Germ-free mice colonized with engineered *Bacteroides thetaiotaomicron* optimized to produce tryptamine (Trp D+) exhibit decreased weight loss and increased mucus release following dextran sodium sulfate treatment when compared with mice colonized with control *B. thetaiotaomicron* (Trp D-). Additional beneficial effects in preventing barrier disruption and lower disease activity index were seen only in female mice, highlighting sex-specific effects of the bacterial metabolite. This study demonstrates potential for the precise modulation of mucus release by microbially produced 5-HT4 GPCR agonist as a therapeutic strategy to treat inflammatory conditions of the GI tract.

INTRODUCTION

The gastrointestinal (GI) tract harbors a diverse microbial community which plays an important role in regulating intestinal physiology and human health (Bhattarai, 2018). These microbial communities are unique among individuals and can in part explain the inter-individual variability in GI physiology. Gut bacteria can communicate with the host via an array of bioactive metabolites in order to influence GI function. We recently described a role for tryptamine produced by bacterial metabolism of dietary tryptophan in increasing intestinal secretion by activating host serotonin receptor 4 (5-HT4R) (Bhattarai et al., 2018). 5-HT4R is a G-protein-coupled receptor (GPCR), which is expressed along the intestinal epithelium and plays an important role in GI physiology beyond regulating intestinal secretion. In this regard, a previous study in transgenic mice has also shown that 5-HT4R is expressed in epithelial goblet cells and pharmacological activation of epithelial 5-HT4R causes goblet cell cavitation suggesting a role of 5-HT4R in luminal mucus release (Hoffman et al., 2012). In addition, epithelial 5-HT4R agonists have also been reported to reduce colitis severity in dextran sodium sulfate (DSS)-treated mice (Spohn et al., 2016) signifying a potential link between epithelial 5-HT4R-induced mucus release and attenuation of colitis severity in mice.

The luminal mucus layer provides a niche for commensal microbial colonization and serves as a carbon source for some gut microbes. In addition to providing a niche for microbial colonization, the mucus layer also serves as a crucial line of defense against invasion and disruption of epithelial layer by pathogens and toxic metabolites. Perturbation of the mucosal barrier as a result of genetic factors or by gut microbiota could therefore allow increased permeability for luminal microbes and their products causing innate immune activation and exacerbation of inflammatory processes such as those observed in patients with inflammatory bowel disease (IBD) (Pullan et al., 1994; Sicard et al., 2017).

Given the importance of mucosal barrier in regulating GI health and preventing inflammatory condition such as IBD (Heazlewood et al., 2008; Johansson et al., 2014; Swidsinski et al., 2007; Van der Sluis et al.,

Figure 1. Tryptamine Evokes Mucus Release Ex Vivo, Which Is Blocked by 5-HT4R Antagonist and Absent in 5-HT4R KO Mice

(A–F) Change in goblet cell cavitation in response to tryptamine, tryptamine + GR-113808, BIMU-8, and Krebs in (A) WT sv/129 and (B) 5-HT4R KO sv/129 mice proximal colon. Representative 40X PAS-H images of WT proximal colon incubated in (C) tryptamine (3 mM), (D) tryptamine (3 mM) + GR (30 nM), (E) BIMU-8 (10 μM), or Kreb's solution (F) for 30 min. Orange circle represents intact goblet cells and while dotted black circle represents cavitated goblet cells. n = 6–7. Data are mean ± SD. *p < 0.05; one-way ANOVA

2006), in this study, we tested the effect of tryptamine, a recently identified bacterially derived 5-HT4R agonist, on mucus release and inflammation in a mouse model of IBD.

RESULTS

Tryptamine Induces Goblet Cell Cavitation by Activating 5-HT4R

The mucosal bilayer within the colon is constantly replenished and maintained through "basal" steady-state release of mucins from epithelial goblet cells and is controlled by several factors such as luminal contents (e.g. polysaccharides), bioactive metabolites (neuropeptides, short chain fatty acids [acetate and butyrate]), neurotransmitters (e.g. 5-HT), and immune factors (inflammatory cytokines) (Barcelo et al., 2000; Burger-van Paassen et al., 2009; Lindén et al., 2008; Mawe and Hoffman, 2013). Besides basal release, a recent study showed that goblet cells can also be stimulated to release mucus through activation of 5-HT4R, a GPCR which is expressed in enterocytes and goblet cells (Hoffman et al., 2012). Therefore, to test if tryptamine, a bacterially derived 5-HT4R-specific agonist (Bhattarai et al., 2018) induces mucus release, we quantified ex vivo mucus release from colonic tissues following treatment with 3 mM tryptamine, a concentration that is comparable to the physiologic concentration of other bacterial metabolites such as short-chain fatty acids (Williams et al., 2014), and compared its efficacy with a known pharmacologic 5-HT4R-agonist, BIMU-8 (10 μM). We found a significant increase in the percentage of cavitated goblet cells following treatment of proximal colonic tissue from conventionally raised 129/Sv wild-type (WT) mice with tryptamine when compared to control (Krebs solution; Figures 1A, 1C–1F, and S1). Tryptamine-induced goblet cell cavitation was significantly reduced by pre-incubating proximal colon tissue with 5-HT4R-antagonist GR-13808 (30 nM) for 10 min to levels similar to the Krebs-only control (Figure 1A). Goblet cell cavitation following treatment with BIMU-8 was comparable to the cavitation induced by tryptamine in WT mice (Figures 1C–1F). Next, to conclusively determine that the tryptamine-induced mucus release was mediated through 5-HT4R, we repeated our ex vivo experiments in 5-HT4R knockout (KO) mice (Figure 1B). Tryptamine and BIMU-8 did not significantly increase goblet cell cavitation compared to control (Krebs) in KO mice unlike the effect seen in WT mice. Together, our data suggest that tryptamine causes goblet cell cavitation and stimulates mucus release in the mouse proximal colon specifically through activation of 5-HT4R. Mucus serves as the first line of defense against luminal factors driving inflammatory responses in the colonic epithelium. Hence, we next determined the physiological relevance of increased mucus release in response to tryptamine in a murine model of IBD.
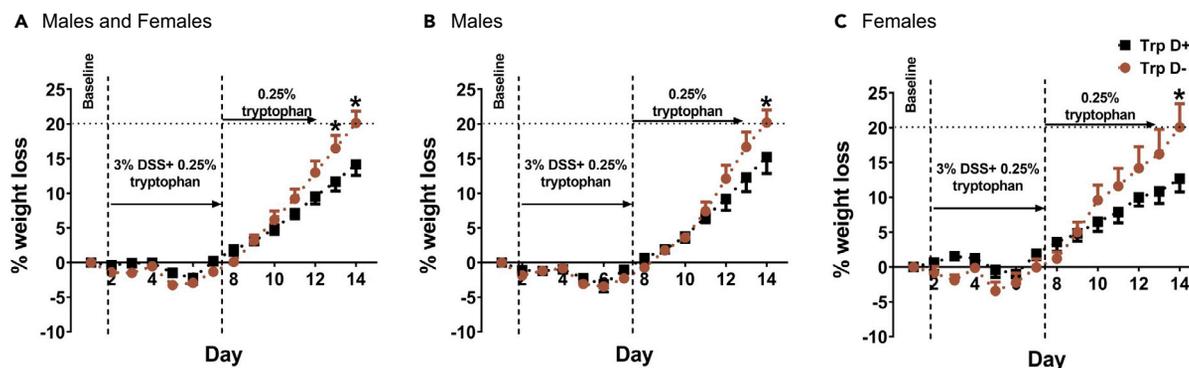
Figure 2. Bacterially Derived Tryptamine Attenuates Weight Loss Following DSS Administration

(A–C) Figures show DSS induced percentage weight loss in both male and female Trp D+ and Trp D monocolonized mice. Dotted line denotes 20% decrease in body weight. n = 12–14 (7–8 males; 5–6 females). Data are mean ± SEM. *p < 0.05; two-way ANOVA with Bonferroni post hoc.

Bacterially Derived Tryptamine Attenuates Colitis Severity in a Murine Model of Inflammatory Bowel Disease

We have previously engineered a *B. thetaiotaomicron* strain to include tryptophan decarboxylase under control of a phage promoter (*B. thetaiotaomicron* Trp D+) to produce tryptamine and show that monocolonization of germ-free (GF) mice with tryptamine producing *B. thetaiotaomicron* Trp D+ results in significantly higher levels of tryptamine and significantly lower levels of tryptophan in the stool when compared to empty vector control (*B. thetaiotaomicron* Trp D) (Bhattarai et al., 2018). We used our previously engineered strains to test if *in vivo* tryptamine production by *B. thetaiotaomicron* Trp D+ strain increased mucus release and was protective against colitis following DSS administration. The experimental outline and study design for bacterial colonization and DSS treatment are highlighted in Figure S2. We used percentage weight loss as the primary surrogate of colitis given that it has been shown to be an objective measure of severity of DSS-induced colitis in mice (Lanka Britto et al., 2019). The optimal concentration of DSS to trigger an inflammatory response has not been well studied in monocolonized mice, and there are scant data in GF mice. Hence, we performed pilot experiments to determine the optimal concentration of DSS that resulted in weight loss in our control *B. thetaiotaomicron* Trp D- monocolonized mice. We found that 1%, 2%, or 2.5% of DSS administration did not result in a significant decrease in body weight (Figure S3). We however found that administration of 3% DSS for 6 days resulted in weight loss in *B. thetaiotaomicron* Trp D- monocolonized control mice (Figure 2A, Table S1). Hence, we used 3% DSS for our experiments. We found that *B. thetaiotaomicron* Trp D+ monocolonized mice showed significantly lower percentage weight loss compared to Trp D- monocolonized mice following treatment with 3% DSS, and this effect was seen in both male (Figures 2B and Table S1A) and female (Figures 2C and Table S1B) monocolonized mice suggesting a protective role for bacterially derived tryptamine in the DSS colitis model. We also performed control experiments to assess the effect of DSS administration in GF mice. However, due to high mortality (≥55% within 3 days of 3% DSS administration) in GF mice compared to monocolonized mice (Figure S4), these experiments had to be discontinued.

The Disease Activity Index (DAI, Table S2) is a severity index often used to assess severity of colitis in DSS-treated mice. In order to determine the severity of colitis, we measured the DAI in *B. thetaiotaomicron* Trp D+ and Trp D- monocolonized mice. We found that while *B. thetaiotaomicron* Trp D+ monocolonized mice had a lower DAI, this was significant only in female mice and not in male mice (Figures 3A–3C) when compared with *B. thetaiotaomicron* Trp D- monocolonized mice. Interestingly, we did not observe any significant difference in histopathological damage score between male or female Trp D+ and Trp D- mice (Figure S5, Table S3). As tryptamine predominantly increases mucus release but does not modify the underlying inflammatory response, the findings above on weight loss, DAI, and histology suggest that tryptamine either helps contain the spread of colitis or blocks initiation of lesion in multiple regions within the colon rather than reduce the severity in individual sites.

Bacterially Derived Tryptamine Reduces DSS-Induced Epithelial Barrier Disruption in Female Mice

The intestinal epithelial layer serves as a physical barrier that prevents inflammation by restricting the unwanted passage of luminal contents, pathogens, and toxic metabolites, which can trigger the intestinal
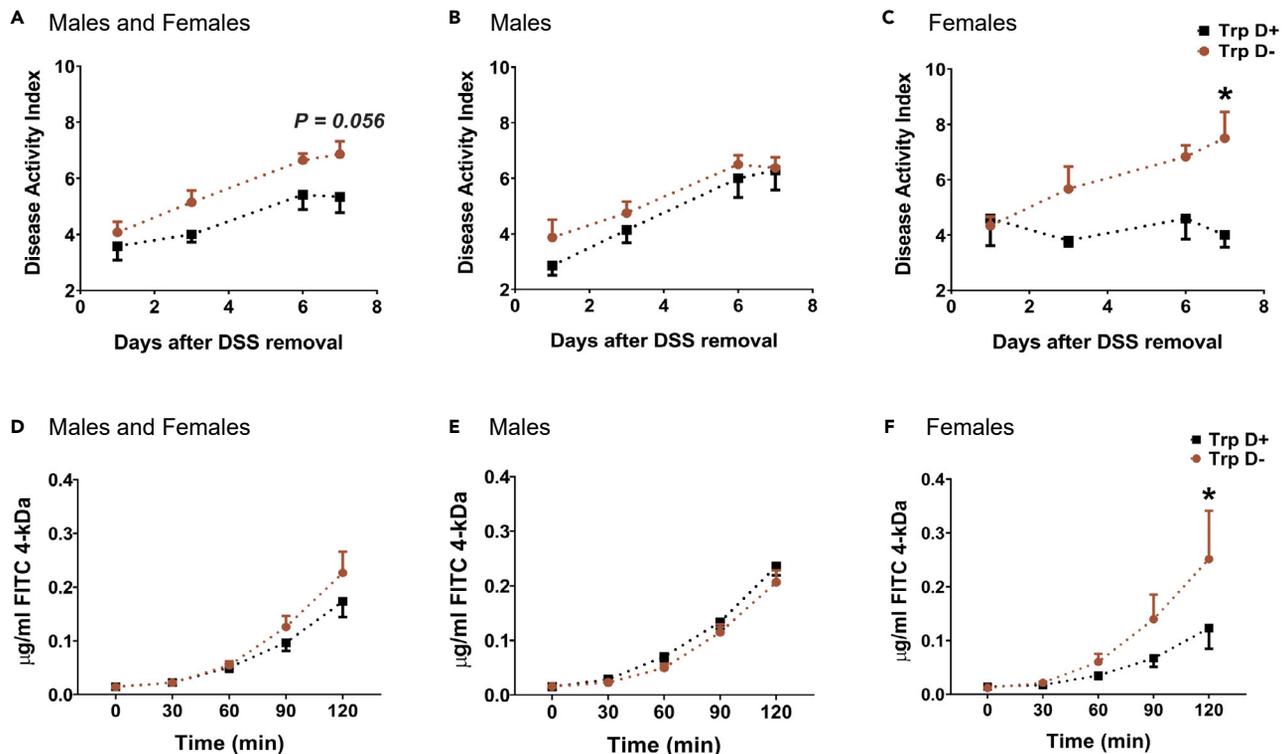
Figure 3. Bacterially Derived Tryptamine Attenuates Colitis Severity as Measured by Disease Activity Index and Epithelial Permeability in Female Mice Following DSS Administration

(A–C) Graphs show change in the DAI over a 7-day period post-DSS administration in both male and female Trp D+ and Trp D monocolonized mice. n = 12–14 (7–8 males; 5–6 females).

(D–F) Graphs highlight change in 4-kDa FITC flux across proximal colon tissue over two hours in both male and female DSS-treated Trp D+ and Trp D monocolonized mice. n = 9 (4–5 males; 4–5 females). Data are mean ± SEM. *p < 0.05; two-way *ANOVA* with Bonferroni post hoc.

immune system. Previous studies have shown that patients with IBD often display disrupted paracellular permeability which may be the initial pathogenic event in IBD (Chang et al., 2017; Lechuga and Ivanov, 2017; McCole, 2014; Söderholm et al., 1999). We therefore tested changes in epithelial permeability following development of DSS colitis in colonic tissues from mice colonized with tryptamine producing *B. thetaiotaomicron* Trp D+ bacteria and control *B. thetaiotaomicron* Trp D- monocolonized. Again, similar to our finding in the DAI, we found that while *B. thetaiotaomicron* Trp D+ monocolonized mice exhibit decreased colonic permeability as indicated by lower 4KDa FITC flux (measure of paracellular permeability), this difference was significant only in female mice but not in male mice (Figures 3D–3F).

To confirm that the capacity to produce tryptamine by the engineered *B. thetaiotaomicron* is not affected by DSS challenge or the biological sex of the recipient mice, we measured tryptamine levels in fecal samples collected 7 days after DSS challenge in *B. thetaiotaomicron* Trp D+ and *B. thetaiotaomicron* Trp D- monocolonized male and female mice. Indeed, Trp D+ monocolonized mice had significantly higher tryptamine levels compared to Trp D- mice. However, there was no difference in tryptamine levels among Trp D+ monocolonized male and female mice (Figures 4A and 4B). This suggests that sex differences observed in the DAI and colonic permeability between Trp D+ and Trp D- mice following DSS treatment were not driven by differences in tryptamine levels and are likely due to host factors.

Bacterially Derived Tryptamine Increases In Vivo Mucus Release following DSS Administration

As we observed increased goblet cell cavitation in response to tryptamine *ex vivo*, we hypothesized that the protective effect of bacterially derived tryptamine to DSS-induced colitis was a result of increased mucus release *in vivo*. Indeed, we found that *B. thetaiotaomicron* Trp D+ monocolonized mice exhibit significantly greater goblet cell cavitation following DSS administration, and this effect was seen in both
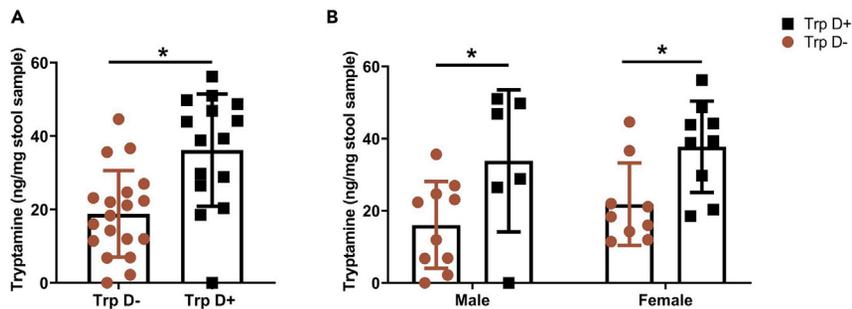
Figure 4. Tryptamine Levels Are Higher in Fecal Samples of DSS Challenged *B. thetaiotaomicron* Trp D + Colonized Mice Compared to *B. thetaiotaomicron* Trp D- Colonized Mice

(A and B) Figures show tryptamine concentration in fecal samples of both DSS challenged male and female Trp D+ and Trp D monocolonized mice. n = 15–19 (6–10 males; 9 females). Data are mean ± SD. *p < 0.05; unpaired t test and two-way *ANOVA* with Bonferroni post hoc.

male and female mice (Figures 5A–5C). This suggests that *in vivo* tryptamine production by gut bacteria increases mucus release, which may play a role in mediating its protective effects in the DSS mouse model of colitis.

DISCUSSION

In this study, we show that colonization of the GI tract by engineered *B. thetaiotaomicron* capable of constitutively producing high levels of tryptamine increases 5-HT4R-dependent mucus release, decreases the severity of colitis, and prevents disruption of the epithelial barrier. The identification of a bacterial metabolite that drives an important host physiologic function can help explain inter-individual variability in susceptibility to inflammatory conditions like IBD, as well as development of a mechanism-based therapeutic approach to treat IBD. Interestingly, tryptamine increases 5-HT4R-dependent mucus release and attenuates weight loss following DSS administration in both sexes. However, the protective effect of bacterially derived tryptamine following exposure to DSS appears more pronounced in female mice as evidenced by significantly lower DAI. This is likely driven by its effect on barrier function and significantly lower intestinal permeability. Our findings highlight the complex interplay between host factors (e.g. estradiol which is known to play a protective role in DSS colitis) and microbiota-derived bioactive compounds that are important in the pathogenesis of chronic diseases.

Luminal tryptamine is produced through enzymatic decarboxylation of tryptophan which is a bacterial function that is present only in a fraction of human gut microbiomes and is rare among bacteria in general (Facchini et al., 2000; Williams et al., 2014). The few bacterial species that have been shown to express native tryptophan decarboxylase include *Clostrodium sporogenes* and *Ruminococcus gnavus* (Williams et al., 2014). Tryptamine production by gut bacteria may represent a selective way for gut microbiota to affect mucus release and utilize mucin as an energy source. For example, the tryptamine producer *R. gnavus* is also an avid mucin degrader that utilizes sialic acid from mucin glycans as a carbon source (Crost et al., 2016). The dual action of tryptamine-producing commensals might therefore be an evolutionary phenomenon for survival and niche establishment. Given the ability to degrade mucin in addition to producing tryptamine, *R. gnavus* strains may not be protective and could even lead to worsening of IBD (Henke et al., 2019). The data presented in our study show that engineering non-mucin degrading strains to produce bacterial GPCR agonists could allow for specifically enhancing mucus release and attenuate inflammation as seen in patients with IBD.

In conclusion, our data show that precise control of tryptamine production in the gut by engineering commensal bacteria can help reinforce the mucus barrier and improve overall colitis burden in response to noxious stimuli in mice. This study is an example of how communication between gut bacteria and the host can be exploited for development of novel therapeutics.

Limitations of the Study

Our study does have a few limitations. While we found an interesting sex dependent difference in the DAI and colonic permeability between *B. thetaiotaomicron* Trp D+ and *B. thetaiotaomicron* Trp D- colonized
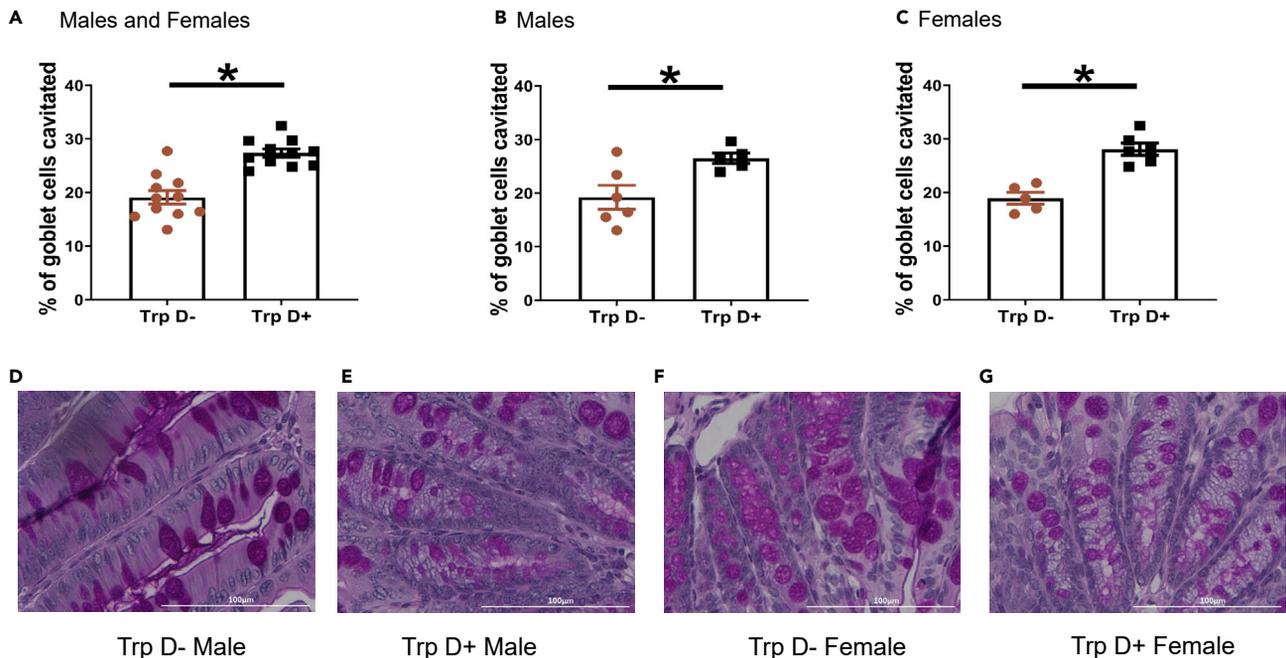
Figure 5. Bacterially Derived Tryptamine Increases In Vivo Mucus Release Following DSS Administration

(A–C) Graphs show difference in goblet cell cavitation post-DSS treatment in both male and female Trp D+ and Trp D monocolonized mice. n = 11 (5–6 males; 5–6 females).

(D–G) Representative 40X PAS-H images of the proximal colon from Trp D- and Trp D+ monocolonized male and female mice subjected to 7 days of DSS challenge. Data are mean $\pm$ SD. *p < 0.05; unpaired t test.

mice subjected to DSS treatment and confirmed that this was not due to differences in bacterial tryptamine production, we have not explored all the host mechanisms that may be driving this sex difference. It is also necessary to emphasize that IBD is a complex multifactorial disorder and as such no single animal model can entirely encapsulate the complex pathophysiology of IBD as seen in humans. In this study, we used the DSS model to test the impact of increased mucus release on inflammation, but further studies in additional models are needed to determine the role of bacterially derived tryptamine in IBD. It is too early to directly extrapolate these findings to humans despite encouraging evidence from our study. Future studies can also help verify whether microbial metabolite mimicry through production of synthetic tryptamine analogs (Abiero et al., 2019) could be used as a potential pharmaceutic modality to improve gut inflammatory conditions.

Resource Availability

Lead Contact

Further information and requests for resources and reagents should be directed to and will be fulfilled by the Lead Contact, Dr. Purna Kashyap (kashyap.purna@mayo.edu).

Materials Availability

This study did not generate new unique reagents or materials. Any materials used in the study will be made available with a material transfer agreement.

Data and Code Availability

This study did not generate novel code, software, or algorithms. No data were generated that required submission in public repositories.

METHODS

All methods can be found in the accompanying Transparent Methods supplemental file.

AUTHORS CONTRIBUTIONS

Y.B., S.J., L.S., and P.C.K. designed the experiments and the overall data analysis; S.J., Y.B., and D.R.L. contributed to the mouse experiments; S.G., D.R.L., Y.B., and S.J. contributed to development of novel histochemistry-based digital image analysis algorithm for assessing mucus release; B.B.W., M.A.F., J.S., S.J., and Y.B. contributed to bacterial engineering and determining culture conditions; R.A.T.M. contributed to tryptamine measurement from fecal pellets; D.R.L. and M.P. contributed to histopathological damage assessment from H&E stained colon slides; and Y.B. and P.C.K. wrote the manuscript with input from all co-authors who read, revised, and approved the manuscript.

DECLARATION OF INTERESTS

P.C.K. reports being on the Advisory Board of Novome Biotechnologies and an *ad hoc* consultant for Pendulum Therapeutics, IP group, and Otsuka Pharmaceuticals. P.C.K. holds patent US20170042860A1 for use of tryptamine producing bacteria ("Transparent Methods for using *Ruminococcus gnavus* or *Clostridium sporogenes* to treat gastrointestinal disorders"), and P.C.K. and Mayo Clinic have a financial interest related to this research. These interests have been reviewed and managed in accordance with Mayo Clinic conflict of interest policies. M.A.F. reports being a co-founder and director of Federation Bio. Y.B. is currently a scientist at Takeda Pharmaceuticals. J.L.S. reports being a founder of Novome Biotechnologies, Inc.

REFERENCES

Abiero, A., Ryu, I.S., Jun Botanas, C., Custodio, R.J.P., Val Sayson, L., Kim, M., Jun Lee, H., Jin Kim, H., Seo, J.-W., Cho, M.C., et al. (2019). Four novel synthetic tryptamine analogs induce head-twitch responses and increase 5-HTR2a in the prefrontal cortex of mice. Biomol. Ther. (Seoul) *28*, 83–91.

Barcelo, A., Claustre, J., Moro, F., Chayvialle, J.A., Cuber, J.C., and Plaisancié, P. (2000). Mucin secretion is modulated by luminal factors in the isolated vascularly perfused rat colon. Gut *46*, 218–224.

Bhattarai, Y. (2018). Microbiota-gut-brain axis: interaction of gut microbes and their metabolites with host epithelial barriers. Neurogastroenterol Motil. *30*, e13366.

Bhattarai, Y., Williams, B.B., Battaglioli, E.J., Whitaker, W.R., Till, L., Grover, M., Linden, D.R., Akiba, Y., Kandimalla, K.K., Zachos, N.C., et al. (2018). Gut microbiota-produced tryptamine activates an epithelial G-protein-coupled receptor to increase colonic secretion. Cell Host Microbe *23*, 775–785.e775.

Burger-van Paassen, N., Vincent, A., Puiman, P.J., van der Sluis, M., Bouma, J., Boehm, G., van Goudoever, J.B., van Seuningen, I., and Renes, I.B. (2009). The regulation of intestinal mucin MUC2 expression by short-chain fatty acids: implications for epithelial protection. Biochem. J. *420*, 211–219.

Chang, J., Leong, R.W., Wasinger, V.C., Ip, M., Yang, M., and Phan, T.G. (2017). Impaired intestinal permeability contributes to ongoing bowel symptoms in patients with inflammatory bowel disease and mucosal healing. Gastroenterology *153*, 723–731.e721.

Crost, E.H., Tailford, L.E., Monestier, M., Swarbreck, D., Henrissat, B., Crossman, L.C., and Juge, N. (2016). The mucin-degradation strategy of Ruminococcus gnavus: the importance of intramolecular trans-sialidases. Gut Microbes *7*, 302–312.

Facchini, P.J., Huber-Allanach, K.L., and Tari, L.W. (2000). Plant aromatic L-amino acid decarboxylases: evolution, biochemistry, regulation, and metabolic engineering applications. Phytochemistry *54*, 121–138.

Heazlewood, C.K., Cook, M.C., Eri, R., Price, G.R., Tauro, S.B., Taupin, D., Thornton, D.J., Png, C.W., Crockford, T.L., Cornall, R.J., et al. (2008). Aberrant mucin assembly in mice causes endoplasmic reticulum stress and spontaneous inflammation resembling ulcerative colitis. PLoS Med. *5*, e54.

Henke, M.T., Kenny, D.J., Cassilly, C.D., Vlamakis, H., Xavier, R.J., and Clardy, J. (2019). *Ruminococcus gnavus,* a member of the human gut microbiome associated with Crohn's disease, produces an inflammatory polysaccharide. Proc. Natl. Acad. Sci. U S A *116*, 12672–12677.

Hoffman, J.M., Tyler, K., MacEachern, S.J., Balemba, O.B., Johnson, A.C., Brooks, E.M., Zhao, H., Swain, G.M., Moses, P.L., Galligan, J.J., et al. (2012). Activation of colonic mucosal 5-HT(4) receptors accelerates propulsive motility and inhibits visceral hypersensitivity. Gastroenterology *142*, 844–854.e844.

Johansson, M.E., Gustafsson, J.K., Holmén-Larsson, J., Jabbar, K.S., Xia, L., Xu, H., Ghishan, F.K., Carvalho, F.A., Gewirtz, A.T., Sjövall, H., et al. (2014). Bacteria penetrate the normally impenetrable inner colon mucus layer in both murine colitis models and patients with ulcerative colitis. Gut 63, 281–291.

Lanka Britto, S., Krishna, M., and Kellermayer, R. (2019). Weight loss is a sufficient and economical single outcome measure of murine dextran sulfate sodium colitis. FASEB Bioadv. 1, 493–497.

Lechuga, S., and Ivanov, A.I. (2017). Disruption of the epithelial barrier during intestinal inflammation: quest for new molecules and mechanisms. Biochim. Biophys. Acta Mol. Cell Res. 1864, 1183–1194.

Lindén, S.K., Florin, T.H., and McGuckin, M.A. (2008). Mucin dynamics in intestinal bacterial infection. PLoS One 3, e3952.

Mawe, G.M., and Hoffman, J.M. (2013). Serotonin signalling in the gut–functions, dysfunctions and therapeutic targets. Nat. Rev. Gastroenterol. Hepatol. 10, 473–486.

McCole, D.F. (2014). IBD candidate genes and intestinal barrier regulation. Inflamm. Bowel Dis. 20, 1829–1849.

Pullan, R.D., Thomas, G.A., Rhodes, M., Newcombe, R.G., Williams, G.T., Allen, A., and Rhodes, J. (1994). Thickness of adherent mucus gel on colonic mucosa in humans and its relevance to colitis. Gut 35, 353–359.

Sicard, J.F., Le Bihan, G., Vogeleer, P., Jacques, M., and Harel, J. (2017). Interactions of intestinal bacteria with components of the intestinal mucus. Front. Cell Infect. Microbiol. 7, 387.

Söderholm, J.D., Peterson, K.H., Olaison, G., Franzén, L.E., Weström, B., Magnusson, K.E., and Sjödahl, R. (1999). Epithelial permeability to proteins in the noninflamed ileum of Crohn's disease? Gastroenterology 117, 65–72.

Spohn, S.N., Bianco, F., Scott, R.B., Keenan, C.M., Linton, A.A., O'Neill, C.H., Bonora, E., Dicay, M., Lavoie, B., Wilcox, R.L., et al. (2016). Protective actions of epithelial 5-hydroxytryptamine 4 receptors in normal and inflamed colon. Gastroenterology 151, 933–944.e3.

Swidsinski, A., Loening-Baucke, V., Theissig, F., Engelhardt, H., Bengmark, S., Koch, S., Lochs, H., and Dörffel, Y. (2007). Comparative study of the intestinal mucus barrier in normal and inflamed colon. Gut 56, 343–350.

Van der Sluis, M., De Koning, B.A., De Bruijn, A.C., Velcich, A., Meijerink, J.P., Van Goudoever, J.B., Büller, H.A., Dekker, J., Van Seuningen, I., Renes, I.B., et al. (2006). Muc2-deficient mice spontaneously develop colitis, indicating that MUC2 is critical for colonic protection. Gastroenterology 131, 117–129.

Williams, B.B., Van Benschoten, A.H., Cimermancic, P., Donia, M.S., Zimmermann, M., Taketani, M., Ishihara, A., Kashyap, P.C., Fraser, J.S., and Fischbach, M.A. (2014). Discovery and characterization of gut microbiota decarboxylases that can produce the neurotransmitter tryptamine. Cell Host Microbe 16, 495–503.

Supplemental Information

Bacterially Derived Tryptamine Increases

Mucus Release by Activating a Host Receptor

in a Mouse Model of Inflammatory Bowel Disease

Yogesh Bhattarai, Si Jie, David R. Linden, Sayak Ghatak, Ruben A.T. Mars, Brianna B. Williams, Meng Pu, Justin L. Sonnenburg, Michael A. Fischbach, Gianrico Farrugia, Lei Sha, and Purna C. Kashyap

Supplemental Information

Figure S1: Measurement of mucus release using PAS-H staining in mouse proximal colon. Related to Figure 1. The 40X raw PAS-H image was deconvoluted in FIJI (Image J v 2.0.0-RC-69/1.52i) software to identify goblet cells within the glandular region of proximal colon. Intensity threshold were manually adjusted to identify mucus containing intact goblet cells and cavitated goblet cells. Percent of cavitated goblet cells was determined using the formula described below.

% of intact goblet cell =

(Low Intensity Threshold (Intact goblet cell) /High Intensity Threshold (Total goblet cell))*100%

% of goblet cell cavitated = 100 - % of intact goblet cell
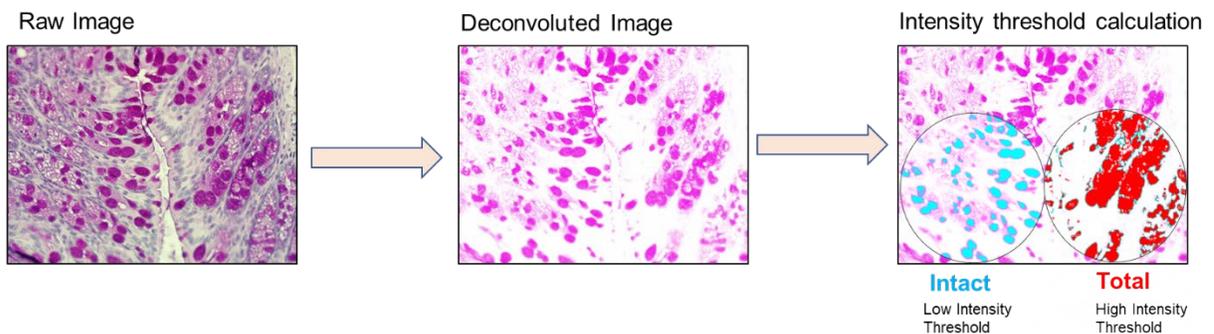
Figure S2: Experimental outline and study design. Related to Figure 2, 3, 4, and 5. (A) 100 µl of frozen *B. thetaiotaomicron* Trp D+/- (*B. theta+/-*) stocks were plated in tryptone yeast extract glucose (TYG) agar plates. After 2 days of incubation, individual bacterial colonies were identified on plates and cultured in a 3ml TYG medium. After 2 days, TYG bacterial cultures were transferred into the gnotobiotic isolator, 300 µl of TYG bacterial solution was then gavaged to GF mice. (B) Drinking water with 0.25% tryptophan was provided to 7-8 week old GF C57BL/6J monocolonized mice followed by 5 days of 3% DSS supplementation to induce colitis. Change in body weight and DAI was measured over the course of 7 days.

A Schematic representation describing *B. theta* Trp D+/- bacteria culture and monocolonization of GF mice
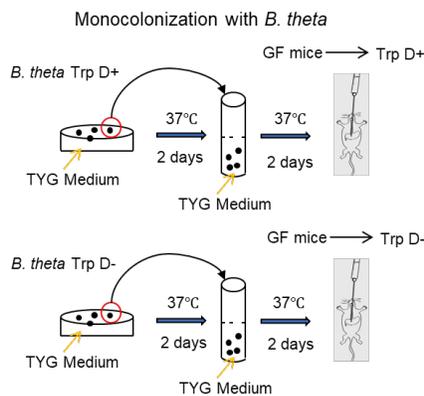
B Timeline describing experimental design for colitis induction, DAI measurement and tissue collection
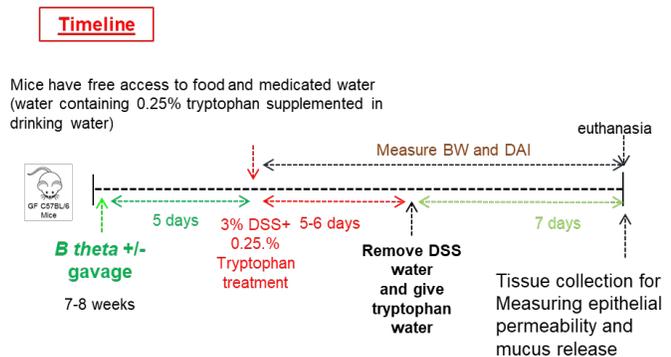
Figure S3: Pilot experiments to determine optimal DSS concentration for induction of colitis in gnotobiotic mice. Related to Figure 2. Figure shows percentage weight loss following administration of 1% (A; n=3-4), 2% (B; n=4) and 2.5% (C; 5-6 males, D; 12-13 females) DSS in mice colonized with *B. thetaiotaomicron* Trp D-. Data are mean±SEM.
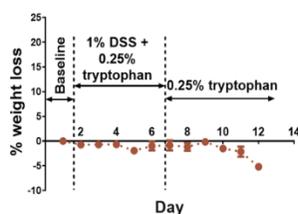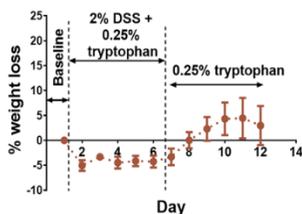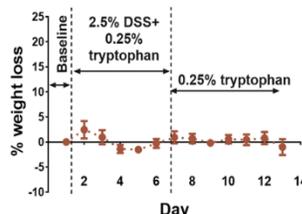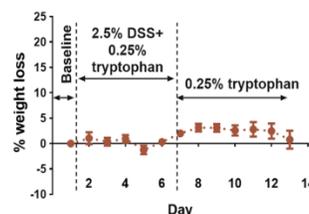
Figure S4: Survival curve for GF and gnotobiotic mice after 3% DSS administration.

Related to Figure 2, 3. Survival curve showing mortality following DSS administration in (A) GF mice and (B) GF mice colonized with *B. thetaiotaomicron* Trp D+/-.
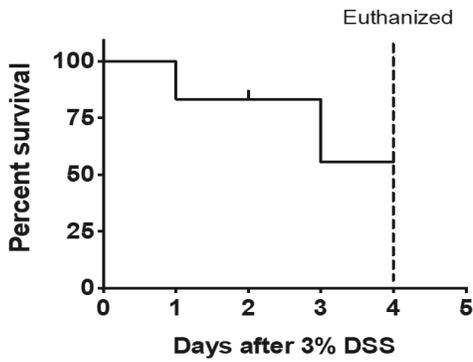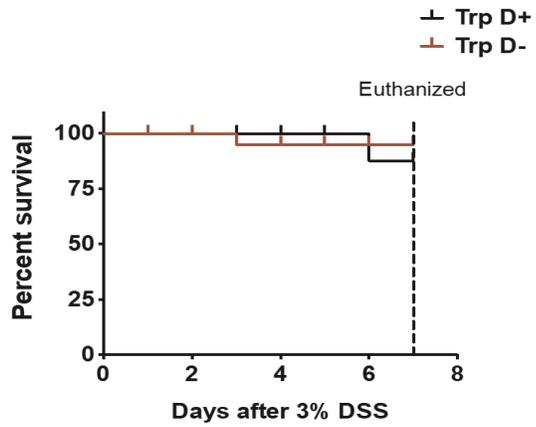
Figure S5: Bacterially-derived tryptamine does not affect severity of inflammation in DSS-challenged mice based on histology. Related to Figure 3. Figures (A-C) quantification of histopathological damage in male and female *B. thetaiotaomicron* Trp D+ and Trp D- monocolonized mice. n=12-13 (7-8 males, 4-6 females). Bars indicate the median and error bars the interquartile range.
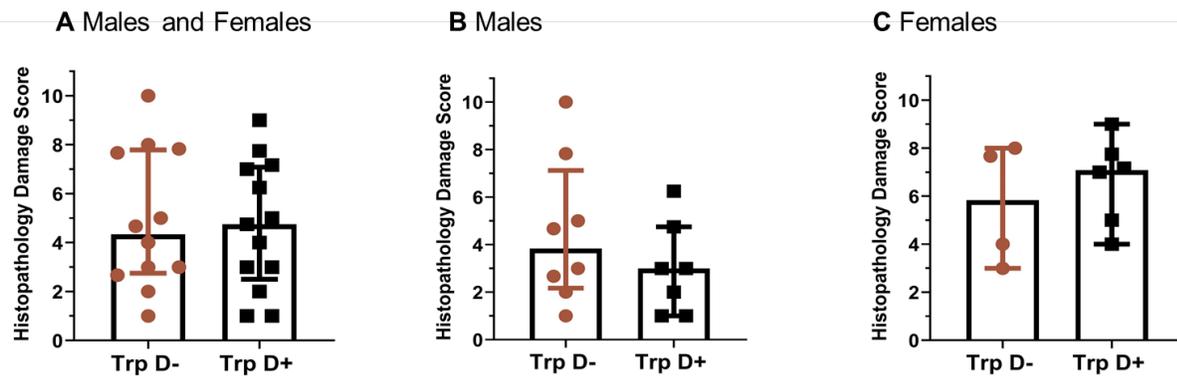
Table S1: Change in body weight after 6 days of 3% DSS administration in Trp D+ and Trp D- monocolonized mice. Related to Figure 2. Change in body weight post DSS administration in (A) male and (B) female *B. thetaiotaomicron* Trp D+ and Trp D- monocolonized mice.

A. Males

Day	Trp D- Mean	Trp D- SEM	n	Trp D+ Mean	Trp D+ SEM	n
BASELINE (DAY 0)	27.625	0.65894	8	27.1571	0.94336	7
1 DAY AFTER DSS	28.1375	0.6716	8	27.4714	1.0087	7
2 DAYS AFTER DSS	27.95	0.63864	8	27.4857	0.94754	7
3 DAYS AFTER DSS	28.25	0.72161	8	27.4143	0.93641	7
4 DAYS AFTER DSS	28.4875	0.74221	8	27.7714	0.94962	7
5 DAYS AFTER DSS	28.575	0.65921	8	28.0229	1.07705	7
6 DAYS AFTER DSS	28.25	0.64003	8	27.4286	0.88498	7
1 DAYS POST WATER SWITCH	27.825	0.65948	8	26.9714	0.93776	7
2 DAYS POST WATER SWITCH	27.1375	0.66088	8	26.6571	0.98823	7
3 DAYS POST WATER SWITCH	26.6375	0.70355	8	26.1286	0.89382	7
4 DAYS POST WATER SWITCH	25.6	0.82245	8	25.3714	0.90599	7
5 DAYS POST WATER SWITCH	24.325	0.97756	8	24.6429	0.8799	7
6 DAYS POST WATER SWITCH	23.075	1.02395	8	23.7857	0.87843	7
7 DAYS POST WATER SWITCH	22.0875	0.89949	8	22.9857	0.89534	7

B. Females

Day	Trp D- Mean	Trp D- SEM	n	Trp D+ Mean	Trp D+ SEM	n
BASELINE (DAY 0)	23.1167	0.56534	6	22.68	0.47896	5
1 DAY AFTER DSS	23.3333	0.73242	6	22.54	0.64467	5
2 DAYS AFTER DSS	23.55	0.53588	6	22.34	0.54461	5
3 DAYS AFTER DSS	23.4	0.5379	6	22.4	0.56833	5
4 DAYS AFTER DSS	23.9	0.54099	6	22.78	0.60778	5
5 DAYS AFTER DSS	23.6167	0.52752	6	22.92	0.72829	5
6 DAYS AFTER DSS	23.1333	0.64533	6	22.26	0.63451	5
1 DAYS POST WATER SWITCH	22.8333	0.55297	6	21.88	0.68659	5
2 DAYS POST WATER SWITCH	21.9667	0.66767	6	21.58	0.42708	5
3 DAYS POST WATER SWITCH	20.9167	0.81544	6	21.2	0.43359	5
4 DAYS POST WATER SWITCH	20.45	0.8582	6	20.88	0.414	5
5 DAYS POST WATER SWITCH	19.8667	0.99488	6	20.4	0.30166	5
6 DAYS POST WATER SWITCH	19.4167	1.13149	6	20.2	0.34496	5
7 DAYS POST WATER SWITCH	18.5167	1.06534	6	19.78	0.34409	5

Table S2: Table highlighting method for disease activity Index (DAI) scoring. Related to Figure 3.

Score	Weight loss	Stool Consistency	Bleeding
0	None	Normal	Normal
1	1-5%		
2	5-10%	Loose stool	Hemoccult +
3	10-20%		Visible blood in stool only
4	>20%	Diarrhea	Gross bleeding (visible)

Table S3: Table highlighting key criteria and method for scoring histopathological damage in DSS challenged *B. thetaiotaomicron* Trp D+/- monocolonized male and female mice. Related to Figure 3.

Histopathology Damage Score Key:	Severity score
Destruction of Normal Architecture	
Normal appearance	0
Hyperplasia	1
Loss of glands in focal spot	2
Loss of glands throughout section	3
Infiltration	
Normal appearance	0
Focal expansion of immune cells	1
Cellulitis in submucosal space	2
Infiltration throughout layers	3
Muscle Thickening	
Normal appearance	0
Slight thickening	1
Thick muscle	2
Maximal thickening	3
Crypt Abscess - neutrophils in crypt	
Not present	0
Present	1
Goblet Cell Depletion	
Normal	0
Depleted	1

Transparent Methods

EXPERIMENTAL MODEL AND SUBJECT DETAILS

Mouse Husbandry and Ethics

Specific pathogen free (SPF) conventionally raised (CR) founder 129/Sv WT and 5-HT4R knockout (KO) mice used for *ex vivo* mucus measurement were previously obtained from our collaborator (Compan et al., 2004). 129/Sv WT and 5-HT4R KO mice were bred, co-housed, and maintained in a micro-isolator caging system using conventional caging and husbandry practices. C57BL/6J germ-free (GF) breeders were obtained from Taconic Farms (Germantown, NY). GF and gnotobiotic C57BL/6J mice were housed within the flexible film vinyl (Class Biologically Clean, Madison, WI) isolators in a temperature-controlled gnotobiotic facility room at 69-70°F in 12 hrs light-dark cycle. Mice were housed in open top cages with autoclaved Sani-Chips bedding and were given ad libitum access to autoclaved diet (Purina Lab diet, 5K67, Collins feed and seed center, Rochester, MN), and autoclaved nano-pure water. Feed and bedding were changed every week or earlier if needed. GF status was confirmed prior to start of experiments with two consecutive negative cultures of fecal pellet, feed and bedding on brain heart infusion (BHI), Sabouraud dextrose, and nutrient media under both anaerobic and aerobic conditions, as well as PCR of 16S rRNA gene using fecal DNA as a template using universal primers and *Turicibacter* primers. GF male and female mice aged 7-8 weeks were used for the study. We were limited by the number of mice we could maintain within the confined space of gnotobiotic isolators, we therefore based our sample size on our previous study using similar methodology (Bhattarai et al., 2018). Mice were randomly assigned within each litter to experimental or controls group. Male and female

mice in each group were co-housed in their respective cages within the gnotobiotic isolator for the entirety the experiment. Since staging mice with in these isolators is challenging and significantly increases both the risk of contamination as well as stress for the mice, female mice were not controlled for estrous cycle in our study. All mice studies were approved by Mayo Clinic Institutional Animal Care and Use Committee (Protocol# A00004100-18) and conducted in compliance with regulatory guidelines.

METHOD DETAILS

Histochemistry to assess *ex vivo* mucus release and histopathological damage in DSS challenged mice

Full-thickness proximal colon segments were obtained 1-2 cm below the cecum. Luminal contents were quickly but gently flushed with chilled Krebs solution (composition in mM/l: 11.5 d-glucose/d-mannitol, 120.3 NaCl, 15.5 NaHCO3, 5.9 KCl, 1.2 NaH2PO4, 2.5 CaCl2·2H2O, and 1.2 MgCl2; pH 7.3–7.4) using a 30 ml syringe hooked to a 200 µl pipette tip. The proximal colon segments were then divided into four equal sections. The sections were equilibrated for 10 minutes in oxygenated 37°C Krebs solution, followed immediately by 30 minutes of incubation under various experimental conditions. After incubation, the tissues were rinsed and placed in an Eppendorf microcentrifuge tube containing 10% neutral buffered formalin at room temperature. Tissues were shipped overnight to the Mayo Clinic histopathology core facility located in Scottsdale, Arizona. Tissues were paraffin-embedded, sectioned, and stained with Periodic Acid-Schiff and hematoxylin (PAS-H) counterstain, and with hematoxylin and eosin (H&E) stain to assess mucus release and histopathological damage post DSS challenge respectively.

In short, the PAS-H protocol involved the following steps. First, cross section paraffinized colonic tissue blocks were sliced into 4 µm thickness. Sliced tissues were then deparaffinized using a series of washes with histological grade xylene (Fisher Scientific #SS32 500, Toronto, Ontario, Canada) and reagent grade ethanol and finally hydrated in distilled water. Tissues were incubated in 1% periodic acid solution for 5 minutes and rinsed with distilled water. Tissues were placed in Schiff's reagent (Fisher Scientific #SS32 500, Toronto, Ontario, Canada) for 45 min and afterwards washed under running tap water for 10 minutes. Tissues were finally counterstained with hematoxylin (Richard Allen Scientific, Ref#7221) for 15 seconds and dehydrated beginning with 95% alcohol and mounted. H&E staining was performed using a standard H&E protocol on tissues from *B. thetaiotaomicron* monocolonized DSS challenged mice. The stained slides were evaluated using a bright-field microscope (Olympus, BX51W1, Olympus Life Science Solutions, Center Valley, PA, USA).

PAS-H images were obtained at 40x magnification and analyzed using FIJI (Image J v 2.0.0-RC-69/1.52i) software. Images were deconvoluted to identify goblet cells within the glandular region of proximal colon. The deconvolution vectors were calculated from PAS-H specific region of interests (ROI) within the individual RGB images. Images were subsequently deconvoluted in accordance with the Beer-Lambert law $I = I_0 \exp(-\varepsilon LC)$, where I is the intensity of the stain as recorded by the charge coupled device camera, I_0 is the intensity of the background white light, ε is the molar attenuation coefficient of the stain, L is the sample thickness and C is the concentration of the stain. The percentage of cavitated and non-cavitated goblet cells was evaluated by the particle analysis function on the PAS channel images after manually adjusting the pixel intensity thresholds to identify mucus-containing intact and mucus-depleted goblet cells. While establishing these methods for assessing

goblet cell cavitation, we found that goblet cell staining in the distal colon was diffuse and harbored poor demarcation compared to proximal colon samples. We thus decided to quantify goblet cell cavitation only in the proximal colon to assess mucus release with greater accuracy and confidence. Representative images and the calculations for this analysis are shown in **Figure S1**.

H&E stained slides were evaluated by a blinded scorer. Histopathological damage assessment as a result of DSS insult was scored based on five histological parameters; destruction of tissue architecture (severity score range: 0-3), immune infiltration (0-3), muscle thickening (0-3), crypt abscess (0-1) and goblet cell depletion (0-1). The severity scores were then summed to get a total damage score. Key criteria for damage scoring and severity scoring are tabulated in **Table S3**.

Generation of bacterial strains and growth conditions

Previously described engineered *Bacteroides thetaiotaomicron* that encodes a phage promoter driving the tryptophan decarboxylase (Trp D+) gene capable of producing tryptamine, and a vector-only control strain of *B. thetaiotaomicron* (Trp D-) were used in this study (Whitaker et al., 2017). Successful integration of the plasmid into the *B. thetaiotaomicron* chromosome was confirmed in the previous study by PCR (Whitaker et al., 2017) and through *in vitro* production of tryptamine in tryptone-yeast extract-glucose (TYG) culture media containing tryptophan (Bhattarai et al., 2018). Bacterial gavage sample were prepared from engineered *B. thetaiotaomicron* Trp D+ and Trp D- frozen stocks from previous study (Bhattarai et al., 2018). Frozen stocks stored in crimp top chromatography vials in -80°C freezer were first slowly thawed in a small container containing sparse amount of dry ice. 100

µl of thawed stock was withdrawn using a tuberculin syringe and streaked on pre-reduced tryptone yeast extract glucose (TYG) agar plates. The plates were incubated inside an anaerobic growth chamber, kept at 37°C, and supplied with 15% CO_2, 5% H_2 and 80% N_2 (Coy Laboratory Products, Grass Lake, MI). After two days of culture, single bacterial colonies were inoculated into liquid TYG culture medium using sterile inoculating loops. After 24 hours of liquid culture, the culture medium was aliquoted into sterile 2 ml cryovials and sealed before removing from the anaerobic chamber to prevent oxygen exposure. The sealed aliquots were transferred into two separate sterile experimental isolators containing GF mice. 300 µl of TYG aliquot containing *B thetaiotaomicron* Trp D+ and Trp D- strains was gavaged into seven to eight weeks old male and female GF mice (**Figure S2A**).

Induction and evaluation of DSS induced colitis in mice

GF mice were co-housed inside the gnotobiotic isolators based on their sex and monocolonized between 7-8 weeks with either tryptamine producing *B. thetaiotaomicron* Trp D+ strain or with *B. thetaiotaomicron* Trp D- control strain. Drinking water was supplemented with 0.25% tryptophan immediately after colonization. After five days of monocolonization, freshly prepared 3% (wt/vol) dextran sulfate sodium salt (DSS, molecular weight 40 kDa, Catalog#42867, Sigma Life Science, USA) was introduced into drinking water to induce colitis. Mice were maintained on 1-3% DSS and 0.25% tryptophan water for a period of 5-6 days. Freshly prepared DSS tryptophan water was switched on day 3 and completely removed by day 5-6. Mice were then continuously maintained on 0.25% tryptophan water for additional 7 days (**Figure S2B**). During this period change in body weight was determined by trained individuals blinded to the treatment groups (**Table S1**). In case body weight loss

exceeded >20% of the initial body weight on 7th day post DSS removal, the protocol was

terminated on 7th day per humane endpoint guidelines set in the IACUC protocol (Mayo Clinic

IACUC Protocol# A00004100-18). Colitis severity was assessed using a disease activity index

(DAI) score, which was determined by calculating sum of scores for change in percentage

weight loss, stool consistency score and hematochezia score. The scoring system for DAI is

presented in **Table S2**.

Tissue preparation

Mice were euthanized by day 7 post DSS administration. Mice were asphyxiated with

CO_2, and euthanasia was confirmed by cervical dislocation. For every mouse, a segment of

proximal colon ~ 2 cm below the cecum was removed. The luminal contents were flushed with

chilled (4°C) Krebs solution. Segment of proximal colon tissue used to analyze ex-vivo

epithelial permeability in Ussing chambers were opened along the mesenteric border. Another

piece of proximal colon tissue was stored in 10% formalin for histochemistry as described

above.

Ussing chamber to measure *ex-vivo* epithelial permeability

To measure change in *ex vivo* epithelial permeability, the opened proximal colon

segment was pinned flat on Sylgard with the mucosa side facing up. Full thickness tissue was

transferred and mounted on an Ussing cassette (Physiologic Instruments, San Diego, CA)

with an aperture of 0.31 cm^2 under a dissecting microscope with fine forceps. The chamber on

the submucosal side was bathed with 4 ml of glucose-containing Krebs solution while the

mucosal side was bathed with 4 ml of mannitol Krebs solution. The Krebs solution was

bubbled with 97% O_2 and 3% CO_2 mixture. Flux of 4 mg/ml 4KDa FITC (Fluorescein isothiocyanate), a measure of paracellular transport, was determined over a period of two hours with readings recorded every 30 minutes.

Tryptamine measurement in fecal samples post DSS challenge

To confirm that engineered *B. thetaiotaomicron* survives DSS challenge and produces tryptamine during the course of the study, tryptamine levels in fecal pellets on the last day of DSS challenge were determined essentially as previously described by Sangwan et al (Sangwan et al., 1998). Briefly, fecal pellet samples were weighed in pre-weighed bead beating tubes filled with ~100 μl of 0.1 mm glass beads. Per mg of fecal pellet 8 μl nanopure water was added and tubes were homogenized using beat beating (40 seconds, 6 meter/second). The tubes were centrifuged at max speed for 10 minutes at 4^oC and 50 μl of cleared extract was transferred to a clean microcentrifuge tube. To this extract 50 μl of assay buffer was added consisting of 5 mM beta-mercaptoethanol, 5 mM thiourea, and 1 mM ethylenediaminetetraacetic acid (EDTA) in 0.1 M sodium phosphate buffer (pH 7.5). Samples were alkalized with 0.2 ml of 4 N NaOH and phase extracted with 350 μl of ethyl acetate. After vortexing and allowing 10 minutes of phase separation, 100 μl of the upper ethyl acetate phase was added to a solvent-compatible 96 well plate and directly subjected to spectrofluorometric fluorescence monitoring in a Biorad Synergy plate reader (excitation 290 nm / emission 360 nm). A tryptamine standard curve was generated by serial dilution of 1 mg/ml tryptamine (Sigma 193747 Sigma-Aldrich Corp., St. Louis, MO, USA) in assay buffer and processed in parallel. Extraction specificity was verified using mixes of tryptophan and tryptamine.

QUANTIFICATION AND STATISTICAL ANALYSIS

Statistical Analysis

All statistical analyses (Student's *t test* and *ANOVA*) were conducted with Prism 7.0a software (GraphPad San Diego, CA, USA). All bar graphs were presented either as Mean ± SD or median ± interquartile range, while line graphs were presented as Mean ± SD. *P* < 0.05 was considered statistically significant.

SUPPLEMENTAL REFERENCES

Bhattarai, Y., Williams, B.B., Battaglioli, E.J., Whitaker, W.R., Till, L., Grover, M., Linden, D.R., Akiba, Y., Kandimalla, K.K., Zachos, N.C.*, et al.* (2018). Gut Microbiota-Produced Tryptamine Activates an Epithelial G-Protein-Coupled Receptor to Increase Colonic Secretion. Cell Host Microbe *23*, 775-785.e775.

Compan, V., Zhou, M., Grailhe, R., Gazzara, R.A., Martin, R., Gingrich, J., Dumuis, A., Brunner, D., Bockaert, J., and Hen, R. (2004). Attenuated response to stress and novelty and hypersensitivity to seizures in 5-HT4 receptor knock-out mice. J Neurosci *24*, 412-419.

Sangwan, R.S., Mishra, S., and Kumar, S. (1998). Direct fluorometry of phase-extracted tryptamine-based fast quantitative assay of L-tryptophan decarboxylase from Catharanthus roseus leaf. Anal Biochem *255*, 39-46.

Whitaker, W.R., Shepherd, E.S., and Sonnenburg, J.L. (2017). Tunable Expression Tools Enable Single-Cell Strain Distinction in the Gut Microbiome. Cell *169*, 538-546.e512.